

See discussions, stats, and author profiles for this publication at: <https://www.researchgate.net/publication/249316611>

Effect of Molecular Weight on the Electrophoretic Deposition of Carbon Black Nanoparticles in Moderately Viscous Systems

ARTICLE in LANGMUIR · JULY 2013

Impact Factor: 4.46 · DOI: 10.1021/la401657d · Source: PubMed

CITATION

1

READS

45

4 AUTHORS:



Satyam Modi

University of Massachusetts Lowell

3 PUBLICATIONS 6 CITATIONS

SEE PROFILE



Artee Panwar

University of Massachusetts Lowell

10 PUBLICATIONS 55 CITATIONS

SEE PROFILE



Joey L. Mead

University of Massachusetts Lowell

98 PUBLICATIONS 671 CITATIONS

SEE PROFILE



Carol M F Barry

University of Massachusetts Lowell

75 PUBLICATIONS 385 CITATIONS

SEE PROFILE

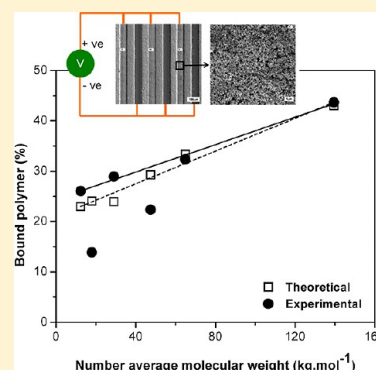
Effect of Molecular Weight on the Electrophoretic Deposition of Carbon Black Nanoparticles in Moderately Viscous Systems

Satyam Modi, Artee Panwar, Joey L. Mead, and Carol M. F. Barry*

NSF Nanoscale Science and Engineering Center for High-Rate Nanomanufacturing, University of Massachusetts Lowell, Lowell, Massachusetts 01854, United States

Supporting Information

ABSTRACT: Electrophoretic deposition from viscous media has the potential to produce in-mold assembly of nanoparticles onto three-dimensional parts in high-rate, polymer melt-based processes like injection molding. The effects of the media's molecular weight on deposition behavior were investigated using a model system of carbon black and polystyrene in tetrahydrofuran. Increases in molecular weight reduced the electrophoretic deposition of the carbon black particles due to increases in suspension viscosity and preferential adsorption of the longer polystyrene chains on the carbon black particles. At low deposition times (≤ 5 s), only carbon black deposited onto the electrodes, but the deposition decreased with increasing molecular weight and the resultant increases in suspension viscosity. For longer deposition times, polystyrene codeposited with the carbon black, with the amount of polystyrene increasing with molecular weight and decreasing with greater charge on the polystyrene molecules. This deposition behavior suggests that use of lower molecular polymers and control of electrical properties will permit electrophoretic deposition of nanoparticles from polymer melts for high-rate, one-step fabrication of nano-optical devices, biochemical sensors, and nanoelectronics.



INTRODUCTION

Since surfaces with micrometer and submicrometer-scale patterns of nanoparticles have potential applications in nanoelectronics,¹ nano-optical devices,² biochemical sensors,^{3,4} and high-density magnetic data storage devices,⁵ numerous methods have been developed to pattern nanoparticles onto substrates. Dip-pen nanolithography,^{6,7} light-based patterning techniques,⁸ electrodeposition with scanning electron microscopy,⁹ and capillary molding¹⁰ provide nanoscale resolution but have less potential as commercial processes. Microcontact printing,¹¹ inkjet printing,¹² screen printing,¹³ and organic vapor jet printing¹⁴ are rapid manufacturing processes which are currently limited to microscale resolution. Electrophoretic^{15,16} and dielectrophoretic^{17,18} deposition processes permit patterning of nanoparticles and can achieve high rates; however, the patterned particles often must be transferred onto a second substrate in a multiple-step process.^{16,17}

Polymer melt-based manufacturing methods, such as injection molding, offer the potential of directly fabricating three-dimensional parts with nanostructured surfaces in a one-step, high-rate, and solventless process. Electrophoretic deposition (EPD) has the potential to produce in-mold assembly of nanoparticles during injection molding. The process is fast, is cost-effective, can be automated as a continuous process on an industrial scale,¹⁹ and is used to "coat" a wide range of materials, including metals, ceramics, and polymers, onto a variety of substrates.²⁰ As mentioned previously, EPD has been used to pattern colloidal gold particles,²¹ silica nanoparticles,²² cadmium selenide nano-

particles,²³ polystyrene particles,²⁴ carbon nanotubes,²⁵ polyaniline,²⁶ and other materials. This electrophoretic deposition, however, was performed from low-viscosity media. Polymer melts are a far more viscous medium, and their viscosity increases with the polymer's molecular weight (i.e., chain length).

Recently, Modi et al.²⁷ have reported the assembly of carbon black particles from moderately viscous suspensions of a polystyrene in tetrahydrofuran. As with other EPD processes, the deposition of the carbon black particles increased with the applied voltage, deposition time, and carbon black concentration in the suspension. Strong polymer–filler interactions, however, caused polystyrene molecules to deposit with the carbon black particles. This codeposition of polystyrene and carbon black affected the deposition rates. The deposition did not increase linearly with applied voltage but exhibited lower deposition rates at high applied voltages. Deposition rates also decreased after deposition times of 5–10 s. Moreover, the voltage or time at which the deposition rate changed decreased with greater suspension concentration. Therefore, the polymer–filler interaction is an important parameter affecting the deposition behavior of polymer and filler systems.

The adsorption of polymer chains on filler particles has widely been observed in preparation of rubber compounds.²⁸ These polymer chains are referred to as "bound rubber". The

Received: May 2, 2013

Revised: June 28, 2013

Published: July 12, 2013



polymer–filler interactions depend on the filler's structure, surface area, and surface activity; the chemical structure of the polymer; and the polymer's macromolecular characteristics such as molecular weight, polydispersity, and branching.²⁸ Carbon black with smaller particle aggregate diameters increased the reinforcement of polybutadiene due to the increased surface area and, thus, the increased level of bound polymer.²⁹ Greater surface activity also provides a greater distribution of highly active sites for the adsorption of polymer segments. For example, the presence of silane groups has increased the bound polymer content of a silica-filled polybutadiene compound compared to that of a carbon black filled system.³⁰ Using an equal loading of the same carbon black particles, Leblanc et al.³¹ found that the bound rubber content was higher for *cis*-polyisoprene than for *cis*-polybutadiene rubber due to the greater flexibility of the *cis*-polyisoprene chains; ethylene-propylene rubber (EPDM) had even less bound rubber because of the reduced frequency of carbon–carbon double bonds. In addition, molecular weight plays an important role in determining polymer–filler interactions. Higher molecular weight polymer chains preferentially adsorb onto the surfaces of filler particles.³² Kida et al.³³ found that the bound rubber content of carbon black-filled polyisoprene systems increased linearly with molecular weight, and Karasek et al.³² observed that the molecular weight of the "unbound polymer" extracted from a carbon black-filled styrene-butadiene compound decreased with increasing bound rubber content. Based on work with a polysiloxane-silica system, Cohen-Addad³⁴ predicted that the bound rubber, BdR, content increases with the number-average molecular weight of the uncured rubber, \bar{M}_n , as

$$BdR = \frac{\sqrt{\bar{M}_0}}{A_0} \cdot \frac{cS_p}{\epsilon_a N_A} \cdot \sqrt{\bar{M}_n} \quad (1)$$

where \bar{M}_0 is the average molecular weight of the skeletal bond, A_0 is the average area of the filler particles associated with one hydrogen bond, c is the particle (filler) concentration, S_p is the specific surface area of the particles, ϵ_a is the numerical factor accounting for chain stiffness and surface coverage, and N_A is the Avogadro number. Moreover, when solution blending carbon black-filled polyisoprene compounds, Kida et al.³³ reported a nonlinear increase in bound rubber content with increasing suspension concentration; this bound rubber content correlated linearly with the greater suspension viscosity at higher molecular weights.

To facilitate in-mold patterning of nanoparticles during injection molding, there is a need to understand the assembly of nanoparticles from viscous media. Thus, the effect of molecular weight on the deposition behavior during the electrophoretic deposition process was investigated using model systems of carbon black and polystyrenes with different molecular weights. The carbon black particles and some polystyrene were assembled on surfaces with microscale patterns (templates) from moderately viscous suspensions of the model systems. The measured surface coverage of the patterns and heights of the deposits were evaluated for the effects of suspension viscosity, bound polymer content, and other factors affecting deposition.

EXPERIMENTAL SECTION

Materials. This investigation was performed using a model system consisting of carbon black particles and polystyrene in tetrahydrofuran

(THF). The carbon black (CB N330, Cabot Corporation) had a reported average particle size of 26–30 nm³⁵ (although the aggregate sizes are larger). Six relatively monodisperse linear polystyrenes reduced the effects of branching and varying molecular weight; the seventh polystyrene had been used in the previous study.²⁷ The weight-average molecular weights, \bar{M}_w ; number-average molecular weights, \bar{M}_n ; and polydispersities, \bar{M}_w/\bar{M}_n , of the polystyrenes are listed in Table 1.^{36,37} The carbon black, polystyrenes, and THF (99.9% reagent grade, Sigma-Aldrich Co.) were used as received.

Table 1. Molecular Weights and Polydispersities of Polystyrene

\bar{M}_w (kg·mol ⁻¹)	\bar{M}_n (kg·mol ⁻¹)	\bar{M}_w/\bar{M}_n	
13.2	12.4	1.06	Sigma-Aldrich Co.
18.1	18.0	1.01	Scientific Polymer Products, Inc.
31.6	29.1	1.09	Sigma-Aldrich Co.
48.1	47.5	1.01	Scientific Polymer Products, Inc.
75.7	64.9	1.17	Scientific Polymer Products, Inc.
151.5	139.5	1.09	Scientific Polymer Products, Inc.
224.4	140.0	1.60	Styron 615APR, Dow Plastics

Concentration Selection. The optimum carbon black concentration for the suspension used in this study was determined experimentally using the polystyrene with weight average molecular weight of 224.4 kg·mol⁻¹; this material had been employed in previous work.²⁷ Six suspensions with polystyrene concentrations of 20, 40, 60, 80, 100, and 160 mg/mL and a constant carbon black concentration of 0.5 mg/mL were prepared. The carbon black was assembled, in a manner discussed later, onto patterned surfaces (templates) using electrophoretic deposition at an applied voltage of 40 V and deposition time of 30 s. The area coverage of carbon black (and polystyrene) on the electrodes was measured. As shown in Figure 1, the area coverage

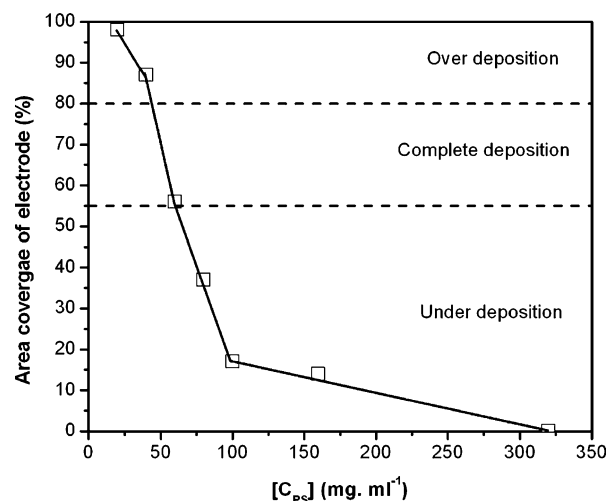


Figure 1. Area coverage of the electrode as a function of polystyrene concentration using a 0.5 mg/mL suspension of carbon black and 224.4 kg·mol⁻¹ molecular weight polystyrene.

of the electrode decreased rapidly with increasing polystyrene concentration. A polystyrene concentration of 60 mg/mL was selected for the molecular weight study because, at that concentration, the area coverage of the electrode was at the line between under deposition and complete deposition - i.e., the electrode was completely covered with carbon black (with overdeposition, the carbon black also deposited on the template substrate).

Preparation and Characterization of the Suspensions. Using a constant concentration of carbon black of 0.5 mg/mL and a constant concentration of polystyrene of 60 mg/mL, six suspensions with

Table 2. Measured and Calculated Parameters of the Suspensions

\bar{M}_w (kg·mol ⁻¹)	η_{PS} (mPa·s)	η (mPa·s)	d (nm)	pH	μ ($\times 10^{-9}$ m ² /Vs)	$1/\kappa$ (nm)	ζ_{PS} (mV)	ζ (mV)	σ (μ S/cm)	q ($\times 10^{-4}$ nm ⁻²)
13.2	0.65	0.63	129	8.5	2.8	53	-0.03	-29	44	1.85
18.1	0.68	0.98	209	8.4	3.7	48	-9.12	-38	35	1.52
31.6	0.70	0.95	376	8.3	1.2	42	-0.02	-13	17	0.28
48.1	0.77	1.43	479	8.5	1.8	53	-0.37	-19	40	0.32
75.7	0.83	1.88	498	8.4	1.6	50	-0.34	-17	14	0.27
151.5	1.00	4.32	510	8.3	0.9	43	-0.23	-9	14	0.15

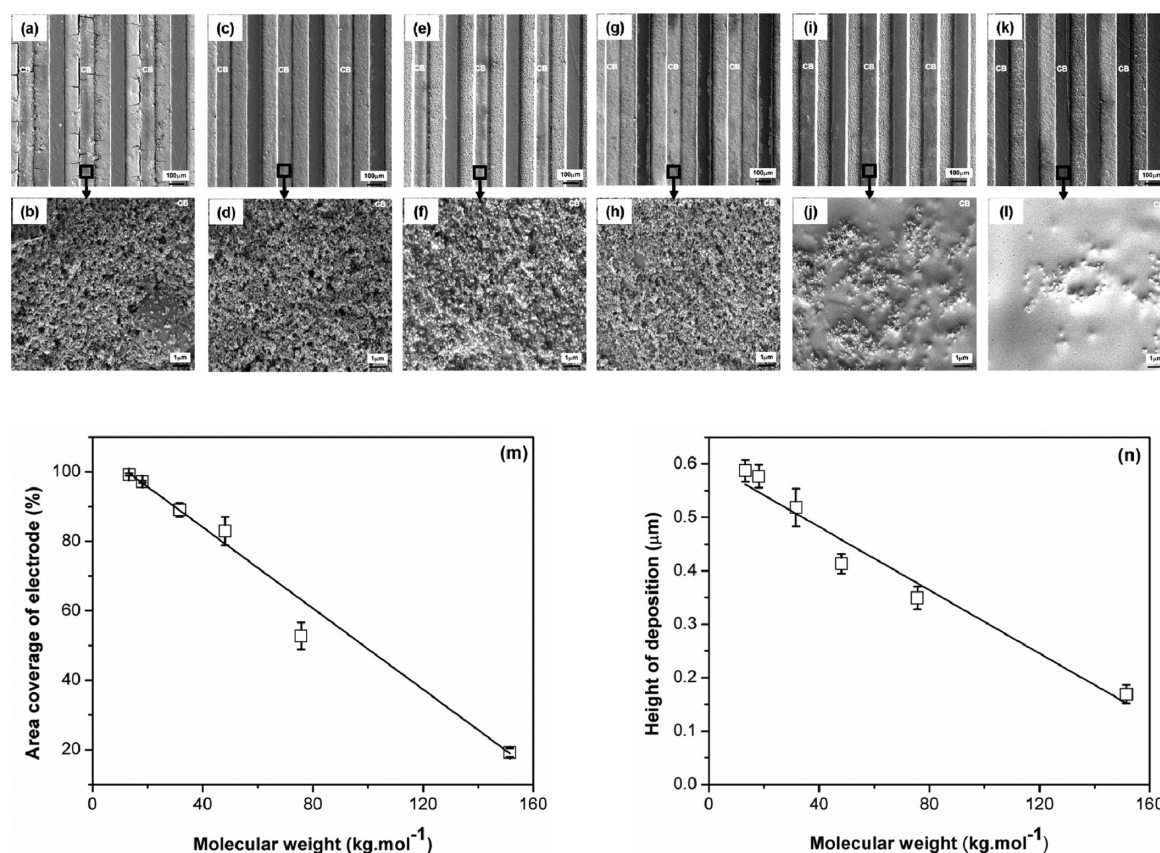


Figure 2. The effect of molecular weight of the template-directed assembly of carbon black using an applied voltage of 40 V and a deposition time of 30 s: (a-b) SEM micrographs for a molecular weight of 13.2 kg·mol⁻¹, (c-d) SEM micrographs for a molecular weight of 18.1 kg·mol⁻¹, (e-f) SEM micrographs for a molecular weight of 31.6 kg·mol⁻¹, (g-h) SEM micrographs for a molecular weight of 48.1 kg·mol⁻¹, (i-j) SEM micrographs for a molecular weight of 75.7 kg·mol⁻¹, (k-l) SEM micrographs for a molecular weight of 151.5 kg·mol⁻¹, (m) plot of area coverage vs molecular weight, and (n) plot of the height of deposition vs molecular weight for a 0.5/60 mg/mL of carbon black (CB)/polystyrene suspension concentration.

polystyrene weight average molecular weights of 13.1, 18.1, 31.6, 48.1, 75.7, and 151.5 kg·mol⁻¹ were prepared. Each suspension was stirred for 24 h using a magnetic stirrer followed by an additional ten minutes of mixing at 3540 rpm using a high-speed mixer (SpeedMixer, Hauschild Engineering).

The measured and calculated parameters of the suspensions are presented in Table 2. The dynamic viscosities of the polystyrene/carbon black suspensions, η , and corresponding polystyrene solutions, η_{PS} , were calculated from the kinematic viscosities measured using an Ubbelohde capillary viscometer (sizes: 0, 25, and 75, Cannon Instrument Co.) in accordance with ASTM D446-07 and ASTM D445-09, respectively. The average carbon black aggregate size, d , was determined using transmission electron microscopy (TEM) (Model: EM400T, Philips); TEM micrographs are provided in Supporting Information, Figure S1. Given that carbon black particles usually do not exist as individual particles - i.e., the smallest entity is the aggregate,³⁵ the aggregate diameters were employed as the particle size in subsequent calculations. The suspension conductivity, σ , and electrophoretic mobility, μ , were measured using a Zetasizer (Zetasizer

Nano series, Model ZEN3600, Malvern Instruments) which employs a combination of laser Doppler velocimetry and phase analysis light scattering in a patented technique called M3-PALS to measure particle electrophoretic mobility.³⁸ The zeta potentials for the polystyrene/carbon black suspensions, ζ , and the polystyrene solutions (with the same concentration of polystyrene), ζ_{PS} , were calculated using the Huckel equation³⁹

$$\mu = \frac{2\epsilon\epsilon_0\zeta}{3\eta} \quad (2)$$

because THF is a polar solvent and the calculated Henry functions, $f(\kappa a)$, ranged from 1.0 to 1.2. The Henry function was determined graphically using calculated " κa " values,⁴⁰ where a was the radius of the carbon black aggregates and κ was the inverse of the double layer thickness; the " κa " values for the suspensions were 2 to 5. The double layer thickness, $1/\kappa$, was calculated using⁴¹

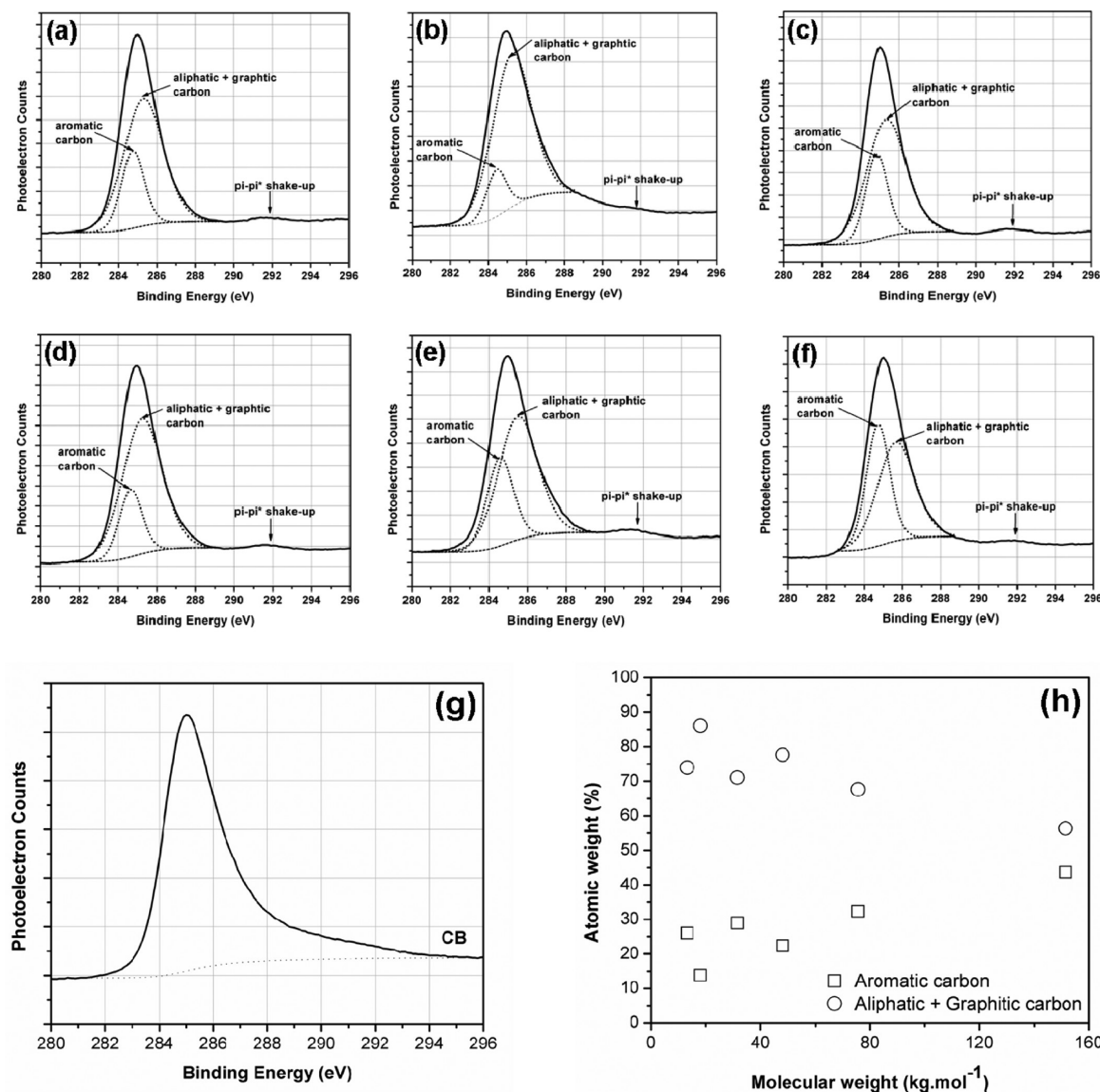


Figure 3. MgK α XPS C1s spectra of the electrodeposited material using an applied voltage of 40 V, a deposition time of 30 s, and 0.5/60 mg/mL carbon black/polystyrene suspension prepared using polystyrene molecular weight of (a) 13.2 kg·mol⁻¹, (b) 18.1 kg·mol⁻¹, (c) 31.6 kg·mol⁻¹, (d) 48.1 kg·mol⁻¹, (e) 75.7 kg·mol⁻¹, (f) 151.5 kg·mol⁻¹, (g) MgK α XPS C1s spectra of carbon black using an applied voltage of 40 V, and a deposition time of 30 s, and (h) plot of the atomic weight percentage vs molecular weight.

$$\frac{1}{\kappa} = \left[\frac{\epsilon \epsilon_0 K T}{2000 e^2 N_A} \right]^{1/2} \quad (3)$$

where ϵ is the dielectric constant of the solvent (7.5), ϵ_0 is the vacuum permittivity ($8.854 \times 10^{-12} \text{ A}^2 \text{ s}^4 \text{ kg}^{-1} \text{ m}^{-3}$), K is the Boltzmann constant ($1.38 \times 10^{-23} \text{ J K}^{-1}$), T is the temperature (298 K), e is the elementary charge ($1.602 \times 10^{-19} \text{ C}$), and N_A is Avogadro's number ($6.022 \times 10^{23} \text{ mol}^{-1}$). The ionic strength, I , was calculated from the measured pH values,⁴² i.e., $I = [\text{H}^+] = 10^{-\text{pH}}$. The pH and double layer thickness values are listed in Table 2. Assuming that the aggregates were spheres, the number of charges per unit area of carbon surface, q , was calculated using⁴³

$$q = \frac{2\zeta\epsilon\epsilon_0}{ed} \quad (4)$$

As shown in Table 2, the conductivity of the suspensions, electrophoretic mobilities, and the resultant zeta potentials (−29 to −14 mV) decreased with increasing polystyrene molecular weight, whereas the measured viscosity and the average carbon black aggregate

size increased with polystyrene molecular weight. The zeta potentials of the suspensions were lower than the −88-mV zeta potential measured for a 0.5 mg/mL suspension of carbon black in THF. Although the 18.1 kg·mol⁻¹ polystyrene had a high zeta potential, another neutrally charged polystyrene with a molecular weight below the critical molecular weight was not available; this second polystyrenes was required to illustrate the effects of molecular weight.

Template-Directed Assembly of Carbon Black from a Moderately Viscous System. The templates used for this work consisted of an interdigitated pattern of 75- μm -wide copper electrodes with a pitch of 175 μm on a 14 mm \times 14 mm polyimide substrate. Prior to electrophoretic deposition, the templates were rinsed five times with acetone and dried with nitrogen. For electrophoretic deposition, the template was immersed at a vertical speed of 86 mm·min⁻¹ into the carbon black-containing suspensions or polystyrene solutions using a dip coater. Once submerged in the suspension or solution, a voltage of 40 V was applied and held for a time ranging from 5 to 30 s. At the end of the deposition time, the voltage was disconnected, and the template was removed from the suspension at the same rate (86 mm/min). After EPD, the template

was dried in air. The EPD process is illustrated in Supporting Information, Figure S2.

Characterization of Electrodeposited Material. 2D optical images of the template after EPD were obtained using a Zeiss Discovery stereomicroscope (Model V20) equipped with an Achromat S 1.0X objective and AxioCam HRc camera. Using image analysis software (Scion Image, Scion Corporation), the images were analyzed to determine the surface coverage of the electrode. The percentage area coverage, A_C , of the electrode was calculated as

$$A_C = \frac{A_{CB}}{A_o} \times 100 \quad (5)$$

where A_{CB} is the area on the electrode occupied by the assembled carbon black particles, and A_o is the area of the electrode. An atomic force microscope (AFM) (Model: XE-150, PSIA) was used to determine the height of the deposited layer. As shown in Supporting Information, Figure S3, a scratch was made perpendicular to the long axis of the electrode; this scratch produced a sharp delineation between the deposited material and the electrode. Using noncontact mode AFM, measurements of these samples were performed using a scan size of $40 \mu\text{m} \times 40 \mu\text{m}$ and a scan rate of 0.20 Hz. The reported height of the deposited layer was determined by averaging the height measured from three separate locations on a particular sample; there were five measurements for each location.

The surface morphology of the deposited carbon black particles was observed using scanning electron microscopy (SEM) (Model: JSM-7401F, JEOL). The chemical composition of the deposit on the electrode surface was investigated using X-ray Photoelectron Spectroscopy (XPS) (ESCALAB MK II, VG Scientific). A MgK α X-ray source was used at a power of 200 W.

RESULTS AND DISCUSSION

Electrophoretic Assembly. Figure 2 presents the SEM micrographs of templates after EPD using a deposition time of 30 s for suspensions having polystyrene molecular weights of 13.2, 18.1, 31.6, 48.1, 75.7, and 151.5 kg·mol⁻¹. As expected, when the electric field was applied, the negatively charged carbon black (and some polystyrene) deposited on the copper fingers connected to the positive electrode, whereas the negative electrodes remained clean. As a result, the copper negative electrodes are darker than the covered positive electrodes (a detailed SEM image is provided in Supporting Information Figure S4). The amount of material deposited on the positive electrodes decreased with increasing weight-average molecular weight. At the higher molecular weights of 151.5 kg·mol⁻¹ (Figures 2k and 2l) and 75.7 kg·mol⁻¹ (Figures 2i and 2j), carbon black particles preferentially deposited onto some of the areas of the electrode with little or no interconnection between the deposited particles. The area coverage was 0 to 55%, and this pattern of deposition was defined as underdeposition. With further decreases in molecular weight - i.e., at 48.1 (Figures 2g and 2h), 31.6 (Figures 2e and 2f), and 18.1 (Figures 2c and 2d) kg·mol⁻¹, sufficient carbon black particles deposited on the electrode to create good interconnections between the particles. This complete deposition produced area coverages of 55 to 90%. In contrast, decreasing the molecular weight to 13.2 kg·mol⁻¹ (Figures 2a and 2b) caused the carbon black to deposit (bridge) between the electrodes. This pattern was defined as overdeposition and was observed when the area coverage of the electrodes was greater than 90%.

As shown in Figures 2m and 2n, the area coverage of the electrode and the height of the deposit on the electrode decreased linearly with increasing weight-average molecular weight. The rates of decrease were 0.6% per kg·mol⁻¹ for area

coverage and 0.002 μm per kg·mol⁻¹ for deposition height; respective coefficients of determination, r^2 , were 0.99 and 0.96. Previous work, however, had shown that this deposit was probably a mixture of carbon black particles and polystyrene.²⁷

Figure 3 presents the XPS C1s spectra of templates after EPD using a deposition time of 30 s, applied voltage of 40 V, and of carbon black/polystyrene suspension concentration of 0.5/60 mg/mL. The XPS was performed to compare the amount of carbon black and polystyrene deposited onto the electrode for the suspensions prepared with polystyrene molecular weights of 13.2, 18.1, 31.6, 48.1, 75.7, and 151.5 kg·mol⁻¹ (Figures 3a–f, respectively). XPS analysis was also performed on a reference sample in which carbon black was assembled on to the template from a suspension of carbon black in THF (Figure 3g). The XPS spectra showed the C1s peak at ~285 eV. For all samples, a peak fitting analysis of the C1s peak was performed by fixing the full width half-maximum (fwhm) range from 2.0 to 2.5 eV. The deconvoluted C1s peaks exhibited two distinct components: the aromatic carbon peak at ~284.6 eV and the graphitic plus aliphatic carbon peak at ~285.0 eV. The peak at ~291.7 eV that appeared in all samples, but not in the carbon black reference, was due to the π – π^* shakeup satellite (which is associated with the presence of localized π electrons in the conjugated phenyl ring of polystyrene⁴⁴). The shakeup satellite has been observed in carbon black samples,^{45,46} but since it was not present in the reference sample, the peak can be used as a clear indicator for the presence of polystyrene in the electrodeposited material. The atomic weight percentage of aromatic carbon peak from polystyrene and aliphatic plus graphitic carbon peak from carbon black derived from the deconvoluted XPS C1s scan were used to estimate the amount of carbon black and polystyrene present in the samples.

As shown in Figure 3h, the atomic weight percentage of aromatic carbon peak generally increased with polystyrene molecular weight, whereas the atomic weight percentage of aliphatic plus graphitic carbon peaks from carbon black decreased with increasing polystyrene molecular weight. The increase in atomic weight percentage of aromatic carbon peak with polystyrene molecular weight suggests that polystyrene molecules deposited on the electrode along with the carbon black particles under the influence of the electric field. Although linear changes in the atomic weight percentages were observed for polystyrene molecular weights of 13.2, 31.6, 75.7, and 151.5 kg·mol⁻¹, inconsistencies occurred with polystyrene molecular weights 18.1 and 48.1 kg·mol⁻¹. With the polystyrene molecular weight of 13.2 kg·mol⁻¹, the atomic weight percentage of aromatic carbon peak was 26% and aliphatic plus graphitic carbon peak was 74%. When the molecular weight of polystyrene was increased to 18.1 kg·mol⁻¹, the atomic weight percentage of aromatic carbon peak, unexpectedly, decreased to 14% and aliphatic plus graphitic carbon peak was increased to 86%. Similarly, for the polystyrene molecular weight of 48.1 kg·mol⁻¹, the atomic weight percentage of aromatic carbon peak (22%) was lower and aliphatic plus graphitic carbon peak (78%) was higher than the respective peaks (29% and 71%) for the polystyrene molecular weight of 31.2 kg·mol⁻¹.

To provide further insight into the electrophoretic deposition from carbon black/polystyrene suspensions, EPD was performed using an applied voltage of 40 V, a 0.5/60 mg/mL of carbon black/polystyrene suspension concentration, and deposition times of 5, 15, and 25 s. Figure 4 presents the XPS

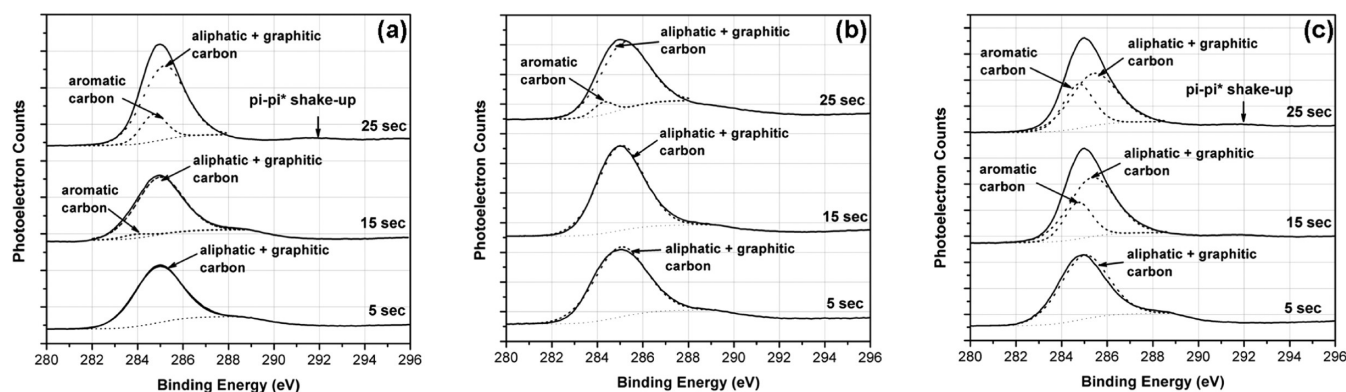


Figure 4. MgK α XPS C1s spectra of the electrodeposited material using an applied voltage of 40 V and 0.5/60 mg/mL carbon black/polystyrene suspension prepared using polystyrene molecular weights of (a) 13.2, (b) 18.1, and (c) 151.5 kg·mol⁻¹.

C1s spectra of the templates after deposition and was performed to compare the amount of carbon black and polystyrene deposited onto the electrode from the suspensions prepared with polystyrene molecular weights of 13.2 kg·mol⁻¹, 18.1 kg·mol⁻¹, and 151.5 kg·mol⁻¹. The graphitic plus aliphatic carbon peak at ~285.0 eV, which is associated with carbon black, was present in all samples; however, the π - π^* shakeup satellite peak at ~291.7 eV and aromatic carbon peak at ~284.6 eV, which indicate the presence of polystyrene, appeared only in samples with higher deposition times and varied with molecular weight. With all molecular weights, increasing deposition time produced the higher deposition of polystyrene molecules, but, at a constant deposition time, the atomic weight percentage of aromatic carbon peak associated with polystyrene varied with molecular weight. Unexpectedly, there was no deposition of polystyrene molecules at the deposition time of 5 s regardless of the polystyrene's molecular weight. At a constant deposition time of 15 s, the atomic weight percentage of aromatic carbon peak for the 13.2 kg·mol⁻¹ sample was 3.85% and for 151.5 kg·mol⁻¹ sample was 27.16%. The atomic weight percentage of the aromatic carbon peak, however, was 0% for the polystyrene molecular weight of 18.1 kg·mol⁻¹. When the deposition time was increased to 25 s, polystyrene deposition was observed with all molecular weights. The atomic weight percentage of aromatic carbon peak for the 18.1 kg·mol⁻¹ molecular weight (7.56%) was lower than the values for molecular weights of 13.2 kg·mol⁻¹ (18%) and 151.5 kg·mol⁻¹ (35.46%).

Since the applied voltage, deposition time, and all geometric features of the electrodes were identical, the decreased rate at which carbon black particles deposited onto the electrode from higher molecular weight suspensions could be due to six possible reasons. First, the presence of a negative charge on the polystyrene molecules could influence the electrophoretic deposition. Polystyrene molecules may have migrated to the template surface under the influence of the applied electric field. Moreover, the charge on the polystyrene may have affected the interaction between the polystyrene and carbon black. Second, the increased suspension viscosity that results from increases in molecular weight may have reduced the mobility of the conductive carbon black particles. Third, the strong polymer–filler interactions between carbon black and polymers containing styrenic groups^{47,48} could allow the polystyrene molecules travel with the carbon black particles to the template surface under the influence of the electric field. Fourth, both deposited molecules have a higher electrical

resistance than the copper electrodes ($1.69 \times 10^{-8} \Omega\cdot\text{m}$),⁴⁹ but polystyrene with an electrical resistance of $5 \times 10^{10} \Omega\cdot\text{m}$ ⁵⁰ is a better insulator than carbon black ($R = 10^{-4}$ to $0.1 \Omega\cdot\text{m}^{51}$). Deposition of both materials should affect the deposition rates. Fifth, the increase in average aggregate size of the carbon black particles with increased polystyrene molecular weight reduces the surface area of the carbon black particles. The larger particles should have a reduction in the charge per unit area on the carbon black surface and particle electrophoretic mobility. Sixth, a decrease in the concentration of carbon black particles near the electrodes, i.e., local depletion, can affect deposition kinetics.⁵²

The polystyrenes used in this work were produced using anionic polymerization.⁵³ Since anions always cannot be removed completely from the polymer chains,⁵⁴ each polystyrene material had a different negative charge (as shown Table 2). So, it was possible for polystyrene molecules to deposit on the template surface under the influence of the applied electric field. To determine whether polystyrene alone migrated in the electric field, electrophoretic deposition was performed using polystyrene solutions (60 mg/mL in THF); the applied voltage was 40 V, and the deposition time was 30 s. Characterization of the templates with AFM showed no deposition on the electrodes. The XPS spectra exhibited very strong Cu2p peaks and a low-intensity C1s peak, both of which are associated with the copper electrode;⁵⁵ once the electrode is covered with carbon black and polystyrene, the intensity of the Cu2p peaks is reduced significantly. (These data are provided in Supporting Information, Figure S5.) Therefore, the negatively charged polystyrene did not undergo electrophoretic deposition in the absence of carbon black.

The presence of a negative charge on the polystyrene molecules may have created a repulsive effect between the negatively charged carbon black particles and the polystyrene. This repulsive effect may have prevented interaction between the polystyrene molecules and carbon black particles causing less neutralization effect on the carbon black surface. Although most of the polystyrenes effectively had zero charge, clear inconsistencies in deposition behavior were observed for suspensions containing polystyrene with molecular weights of 18.1 and 48.1 kg·mol⁻¹. For both materials, atomic weight percentages of the aromatic carbon peak and the graphitic plus aliphatic carbon peak were, respectively, less than and greater than the trends for the rest of polystyrene/carbon black suspensions (Figure 3h). As shown in Table 2, the 18.1 kg·mol⁻¹ molecular weight polystyrene produced zeta poten-

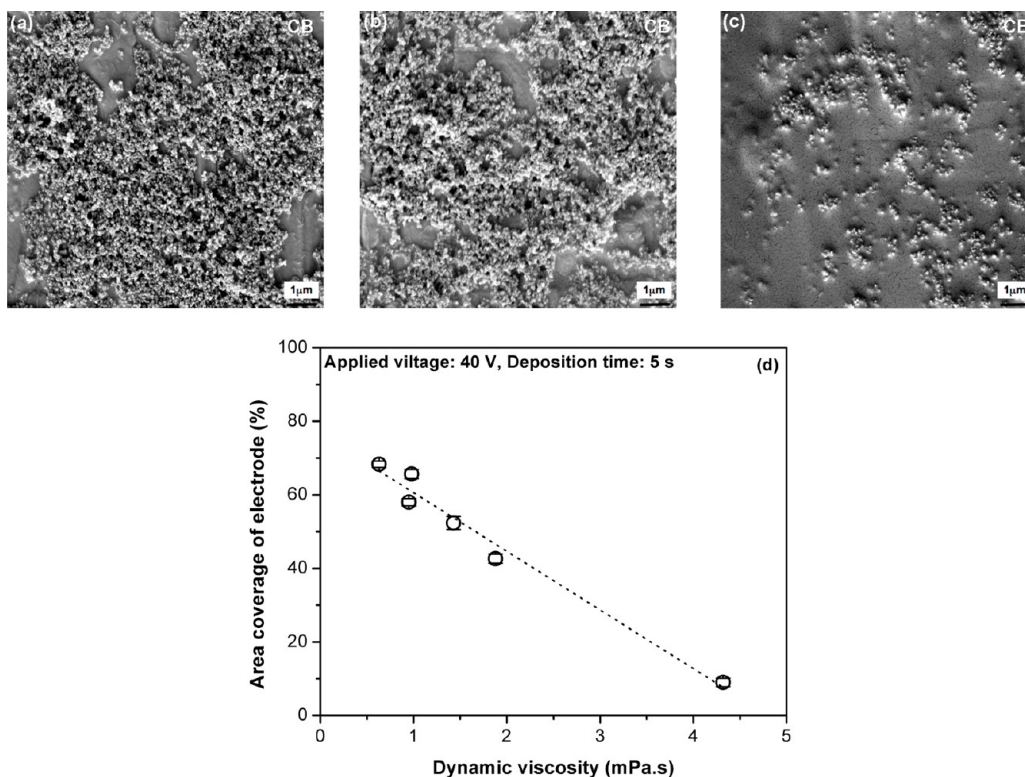


Figure 5. The effect of viscosity of the template-directed assembly using an applied voltage of 40 V and a deposition time of 5 s: (a) SEM micrographs for a molecular weight of 13.2 kg·mol⁻¹, (b) SEM micrographs for a molecular weight of 18.1 kg·mol⁻¹, (c) SEM micrographs for a molecular weight of 151.5 kg·mol⁻¹, and (d) plot of area coverage vs dynamic viscosity for a 0.5/60 mg/mL carbon black/polystyrene suspension.

tials in the polystyrene solution (−9.12 mV) and the carbon black/polystyrene suspension (−38 mV) that were much greater than the zeta potentials produced by the other polystyrenes. Corresponding zeta potentials (−0.37 mV and −19 mV) for the 48.1 kg·mol⁻¹ molecular weight polystyrene, however, were not sufficiently greater than the zeta potentials for the other polystyrenes to explain the inconsistent deposition behavior. The higher charge per unit area of carbon black surface of 1.52×10^{-4} and 0.32×10^{-4} nm² for the 18.1 and 48.1 kg·mol⁻¹ molecular weight polystyrenes, respectively, could also not fully account for the differences in deposition behavior. Electrophoretic mobility values, in which the zeta potential was corrected for molecular weight-induced increases in viscosity, were 12 to 50% greater for the polystyrene with both molecular weights (18.1 and 48.1 kg·mol⁻¹). These differences suggested that the negative charge on the polystyrene reduced the interaction between the polystyrene molecules and carbon black particles. As a result, carbon black was able to deposit on the electrode with 18.1 kg·mol⁻¹ molecular weight polystyrene until the deposition time exceeded 15 s (Figure 4b), and even with a deposition time of 30 s, the deposit was primarily carbon black (Figure 3b). Due to its lower charge, this effect was less pronounced for the 48.1 kg·mol⁻¹ molecular weight polystyrene.

If the charge repulsion between two species is too great, there may be no deposition.¹⁹ This concept was investigated using a polystyrene with a weight-average molecular weight of 8.4 kg·mol⁻¹ and zeta potential of −30.63 mV in a THF solution. When the 0.5/60 mg/mL carbon black/polystyrene suspension underwent template directed electrophoretic deposition using an applied voltage of 40 V and deposition time of 30 s, the area coverage on the electrode was ~70%. In

comparison, the area coverage was 99.24% and 97.14%, respectively, with the 13.2 and 18.1 kg·mol⁻¹ molecular weight polystyrenes. The decrease in the area coverage of the electrode with the greater negative charge on polystyrene molecules suggests that stronger repulsive forces between the negatively charged polystyrene and carbon black particles was not overcome by the electrophoretic forces. Therefore, this repulsive force hindered the deposition of the carbon black particles in EPD.

Given the lack of polystyrene deposition at low deposition times, the effects of viscosity were investigated using an applied voltage of 40 V, deposition time of 5 s, and 0.5/60 mg/mL of carbon black/polystyrene suspension concentration. Figures 5a–5c present the SEM micrographs of the templates after EPD using suspensions with polystyrene molecular weight suspensions of 13.2, 18.1, and 151.5 kg·mol⁻¹, respectively. In case of the 13.2 kg·mol⁻¹ molecular weight sample, the dynamic viscosity of the suspension was 0.63 mPa·s, and the area coverage of the electrode was 68%. Increasing the molecular weight to 151.5 kg·mol⁻¹ increased the dynamic viscosity to 4.32 mPa·s and reduced the area coverage of the electrode to 9%. As shown in Figure 5d, the coverage of the electrode with carbon black decreased linearly with increasing dynamic viscosity of the suspensions. The rate of decrease was 15.9% per mPa·s (the coefficient of determination was 0.97). This behavior suggests that the increased viscosity of the suspensions decreased the mobility of the carbon black particles and, so, reduced the overall deposition. The results also are consistent with Jean's findings⁵⁶ that increased suspension viscosity reduced the electrophoretic mobility of aluminum oxide particles and silicon carbide whiskers (viscosity was increased

by decreasing the isopropanol-to-water ratio of the suspension medium).

The amount of bound polymer deposited on the patterned surface was determined experimentally using the XPS results obtained for samples with deposition times of 30 s. Since XPS can measure only to a 3–5 nm depth into the deposits, these measurements reflect the composition at the surface of the deposit. The theoretical amount of bound polymer deposited on the electrodes was calculated using the Cohen-Addad equation.³⁴ For polystyrene,⁵⁷ $[-CH_2-CH(C_6H_5)-]_n$, two skeletal bonds comprise the repeat unit with a molecular weight of $0.105 \text{ kg}\cdot\text{mol}^{-1}$; hence, M_o is $0.0525 \text{ kg}\cdot\text{mol}^{-1}$. The numerical factor accounting for chain stiffness and surface coverage, ϵ_a was assumed to be 0.35. Previous work²⁸ with the same grade of carbon black (N330) provided the average area of the carbon black particles associated with one hydrogen bond, A_o (50.5 nm^2), and the specific surface area of the particles, S_p , was estimated from the diameter of the carbon black particles (aggregates). The particle (filler) concentration, c , was 0.0083 g/g . As shown in Figure 6, the theoretically

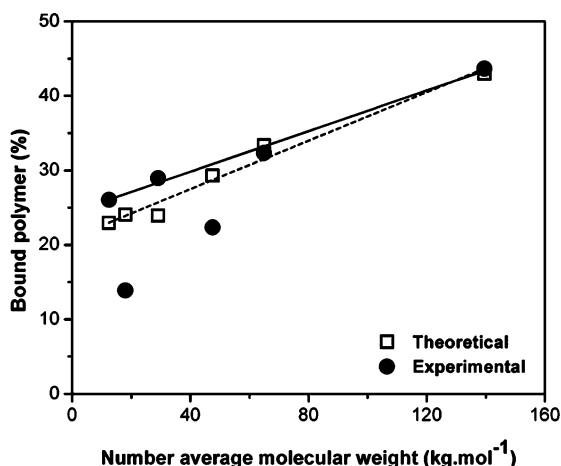


Figure 6. The effect of number-average molecular weight of polystyrene on the experimentally determined and theoretically calculated bound polymer based on results from deposition times of 30 s.

determined amount of bound polymer increased linearly with number-average molecular weight. The experimentally determined amount of bound polymer generally exhibited the same trend, but the polystyrenes with weight-average molecular weights of 18.1 and $48.1 \text{ kg}\cdot\text{mol}^{-1}$ produced lower-than-expected amounts of bound polymer during EPD. These reductions in the bound polymer content correlate with the presence of higher negative charge on these polystyrene molecules. The charges probably hindered adsorption of the polystyrene molecules on the carbon black particles.

Figure 7 presents the effect of deposition time on the area coverage of the electrode for suspensions prepared with 18.1 and $151.5 \text{ kg}\cdot\text{mol}^{-1}$ molecular weight polystyrenes. As in prior work,²⁷ the rate of the area coverage increase was not linear. The area coverage of the electrode increased rapidly at shorter deposition times, but the rate of deposition was lower at longer deposition times. When the polystyrene molecular weight was $18.1 \text{ kg}\cdot\text{mol}^{-1}$, the area coverage of electrode initially increased at the rate of 13% per second, whereas for the deposition times greater than 5 s, the increase in area coverage was significantly lower at 0.97% per second. Similar deposition behavior was

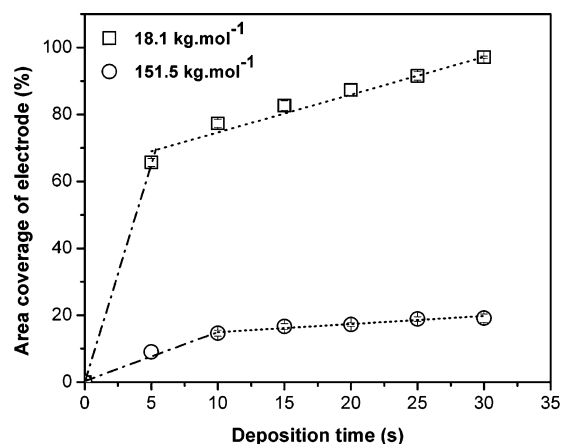


Figure 7. The effect of deposition time on the area coverage of the electrode using an applied voltage of 40 V and 0.5/60 mg/mL carbon black/polystyrene suspension prepared using polystyrenes with molecular weights of 18.1 and $151.5 \text{ kg}\cdot\text{mol}^{-1}$.

observed for the polystyrene with a molecular weight of $151.5 \text{ kg}\cdot\text{mol}^{-1}$; however, the area coverage of electrode first increased linearly at slower rate of 1.47% per second, and after 10 s, the deposition rate decreased to 0.22% per second. The change in deposition rate did not correlate with the deposition of polystyrene. XPS C1s spectra showed that there were no depositions of the $18.1 \text{ kg}\cdot\text{mol}^{-1}$ molecular weight polystyrene molecules at deposition times of 5, 10, and 15 s, but the deposition rate decreased after 5 s. The $151.5 \text{ kg}\cdot\text{mol}^{-1}$ molecular weight polystyrene deposited on the electrodes after 5 s of deposition time, whereas the deposition rate decreased after 10 s. The decreases in the rate of area coverage could have resulted from the insulation effect created by the deposition of less-conductive carbon black particles and, with longer deposition times, codeposition carbon black particles with bound polystyrene. This coverage can increase the electrical resistance and, so, decrease the electric field strength and reduce particle velocity.^{48,58,59} In polymer systems like toners, decreases in electrophoretic mobility have been attributed due to partial covering of the carbon black particles' surface with polystyrene and competition between the carbon black and polystyrene for ions.⁶⁰ A decreased concentration of carbon black particles in the vicinity of electrodes also may have contributed to the reduction in deposition.^{43,48} The linear increases in the deposition rates after the deposition time of 5 s for $18.1 \text{ kg}\cdot\text{mol}^{-1}$ and 10 s for $151.5 \text{ kg}\cdot\text{mol}^{-1}$, however, suggest that the local depletion of carbon black particles near the electrodes may not have occurred in this work.

Carbon black particle (aggregate) size also increased with polystyrene molecular weight. These larger aggregates may have contributed to the reduction in particle mobility with higher molecular weight polystyrenes. The corresponding decreases in deposition with increases in particle size, however, correlated with increases in suspension viscosity. The deposition decreased slowly when the weight-average molecular weight was less than the critical molecular weight ($\sim 35 \text{ kg}\cdot\text{mol}^{-1}$) and much faster for weight-average molecular weights greater than the critical molecular weight. The critical molecular weight is associated with the onset of polymer chains entanglement which significantly increases viscosity.⁵⁴

CONCLUSIONS

The effect of polymer molecular weight on deposition behavior was investigated for electrophoretic deposition from moderately viscous suspensions. Increases in molecular weight reduced the electrophoretic deposition of the carbon black particles due to (1) increases in suspension viscosity and (2) preferential adsorption of the longer polystyrene chains on the carbon black particles. At low deposition times (≤ 5 s), only carbon black deposited onto the electrodes, but the deposition decreased with increasing molecular weight and the resultant increases in suspension viscosity. With longer deposition time (> 5 s), the polystyrene codeposited with the carbon black. The amount of deposited polystyrene increased with molecular weight and decreased with higher charge on the polystyrene molecules. For a polystyrene having a molecular weight of $18.1 \text{ kg} \cdot \text{mol}^{-1}$ and zeta potential of -9.12 mV , only carbon black deposited for the first 15 s of EPD. Excessive charge on the polystyrene ($\zeta = -30 \text{ mV}$), however, reduced overall deposition. The insulating effect created by the deposition of less conductive carbon black particles on the copper electrodes reduced the deposition rate after the electrode was covered with particles. The overall behavior suggests that by using lower molecular polymers, controlling the electrical properties of the polymer and nanoparticles, and employing shorter deposition times nanoparticles can be electrophoretically deposited from the viscous polymer systems, like polymer melts. This process could be extended for the high-rate fabrication of nano-optical devices, biochemical sensors, and nanoelectronics using polymer melt-based processes like injection molding.

ASSOCIATED CONTENT

Supporting Information

TEM images showing the effect of polystyrene molecular weight on carbon black dispersion; a schematic showing electrophoretic assembly of the carbon black-polystyrene system on a patterned surface; AFM images showing measurement of the carbon black deposition height; SEM micrographs detailing the template-directed assembly of the carbon black and polystyrene on the templates; and an AFM image of the electrode after EPD and $\text{MgK}\alpha$ XPS Cu spectra of the material deposited on the electrode using EPD. This material is available free of charge via the Internet at <http://pubs.acs.org>.

AUTHOR INFORMATION

Corresponding Author

*Phone: (001) 978-934-3436. Fax: (001) 978-934-4056. E-mail: Carol_Barry@uml.edu.

Notes

The authors declare no competing financial interest.

ACKNOWLEDGMENTS

This research was supported by the National Science Foundation (NSF grant number: EEC-0832785) under the Nanoscale Science and Engineering Centers program. The authors also thank Dr. Bridgette Budhlall for her assistance.

REFERENCES

(1) Cui, Y.; Bjork, M. T.; Liddle, J. A.; Sonnichsen, C.; Boussert, B.; Alivisatos, A. P. Integration of colloidal nanocrystals into lithographically patterned devices. *Nano Lett.* **2004**, *4*, 1093–1098.

(2) Wei, Q.-H.; Su, K.-H.; Durant, S.; Zhang, X. Plasmon resonance of finite one-dimensional Au nanoparticle chains. *Nano Lett.* **2004**, *4*, 1067–1071.

(3) Andersson, H.; Van der Wijngaart, W.; Stemme, G. Micro-machined filter-chamber array with passive valves for biochemical assays on beads. *Electrophoresis* **2001**, *22*, 249–257.

(4) Velev, O. D.; Kaler, E. W. In situ assembly of colloidal particles into miniaturized biosensors. *Langmuir* **1999**, *15*, 3693–3698.

(5) Hagionoya, C.; Ishibashi, M.; Koike, K. Nanostructure array fabrication with a size-controllable natural lithography. *Appl. Phys. Lett.* **1997**, *71*, 2934–2936.

(6) Ginger, D. S.; Zhang, H.; Mirkin, C. A. The evolution of dip-pen nanolithography. *Angew. Chem., Int. Ed.* **2004**, *43*, 30–45.

(7) Salaita, K.; Wang, Y.; Mirkin, C. A. Applications of dip-pen nanolithography. *Nat. Nanotechnol.* **2007**, *2*, 145–155.

(8) Rogers, J. A.; Paul, K. E.; Jackman, R. J.; Whitesides, G. M. Using an elastomeric phase mask for sub-100 nm photolithography in the optical near field. *Appl. Phys. Lett.* **1997**, *70*, 2658–2660.

(9) Borgwarth, K.; Rohde, N.; Ricken, C.; Hallensleben, M. L.; Mandler, D.; Heinze, J. Electroless deposition of conducting polymers using the scanning electrochemical microscope. *Adv. Mater.* **1999**, *11*, 1221–1226.

(10) Park, M. J.; Choi, W. M.; Park, O. O. Patterning polymer light-emitting diodes by micromolding in capillary. *Curr. Appl. Phys.* **2006**, *6*, 627–631.

(11) Perl, A.; Reinhoudt, D. N.; Huskens, J. Microcontact printing: Limitations and achievements. *Adv. Mater.* **2009**, *21*, 2257–2268.

(12) Kordás, K.; Mustonen, T.; Tóth, G.; Jantunen, H.; Lajunen, M.; Soldano, C.; Talapatra, S.; Kar, S.; Vajtai, R.; Ajayan, P. M. Inkjet printing of electrically conductive patterns of carbon nanotubes. *Small* **2006**, *2*, 1021–1025.

(13) Pardo, D. A.; Jabbour, G. E.; Peyghambarian, N. Application of screen printing in the fabrication of organic light-emitting devices. *Adv. Mater.* **2000**, *12*, 1249–1252.

(14) Sun, Y.; Shtein, M.; Forrest, S. R. Direct patterning of organic light-emitting devices by organic-vapor jet printing. *Appl. Phys. Lett.* **2005**, *86*, 113504–1–113504–3.

(15) Kamat, P. V.; Thomas, K. G.; Barazzouk, S.; Girishkumar, G.; Vinodgopal, K.; Meisel, D. Self-assembled linear bundles of single wall carbon nanotubes and their alignment and deposition as a film in a dc field. *J. Am. Chem. Soc.* **2004**, *126*, 10757–10762.

(16) Wei, M.; Tao, Z.; Xiong, X.; Kim, M.; Lee, J.; Somu, S.; Sengupta, S.; Busnaina, A.; Barry, C.; Mead, J. Fabrication of patterned conducting polymers on insulating polymeric substrates by electric-field-assisted assembly and pattern transfer. *Macromol. Rapid Commun.* **2006**, *27*, 1826–1832.

(17) Shen, J.; Wie, M.; Busnaina, A.; Barry, C.; Mead, J. Directed assembly of conducting polymers on sub-micron templates by electrical fields. *Mater. Sci. Eng., B* **2013**, *178*, 190–201.

(18) Bhatt, K. H.; Velev, O. D. Control and modeling of the dielectrophoretic assembly of on-chip nanoparticle wires. *Langmuir* **2004**, *20*, 467–476.

(19) Besra, L.; Liu, M. A review on fundamentals and applications of electrophoretic deposition (EPD). *Prog. Mater. Sci.* **2007**, *52*, 1–61.

(20) Heavens, S. N. In *Advance Ceramic Processing and Technology*; Binner, J. G. P., Ed.; Noyes Publications: Park Ridge, NJ, 1990; Vol. 1, pp 255–281.

(21) Bailey, R. C.; Stevenson, K. J.; Hupp, J. T. Assembly of micropatterned colloidal gold thin films via microtransfer molding and electrophoretic deposition. *Adv. Mater.* **2000**, *12*, 1930–1934.

(22) Xiong, X.; Makaram, P.; Busnaina, A.; Bakhtari, K.; Somu, S.; McGruer, N. Large scale directed assembly of nanoparticles using nanotrench templates. *Appl. Phys. Lett.* **2006**, *89*, 193108–1–193108–3.

(23) Zhang, Q.; Xu, T.; Butterfield, D.; Misner, M. J.; Ryu, D. Y.; Emrick, T.; Russell, T. P. Controlled placement of CdSe nanoparticles in diblock copolymer templates by electrophoretic deposition. *Nano Lett.* **2005**, *5*, 357–361.

(24) Trau, M.; Saville, D. A.; Aksay, I. A. Assembly of colloidal crystals at electrode interfaces. *Langmuir* **1997**, *13*, 6375–6381.

- (25) Mazurenko, I.; Etienne, M.; Tananaiko, O.; Urbanova, V.; Zaitsev, V.; Walcarius, A. Electrophoretic deposition of macroporous carbon nanotube assemblies for electrochemical applications. *Carbon* **2013**, *53*, 302–312.
- (26) Kumar, A.; Kazmer, D. O.; Barry, C. M. F.; Mead, J. L. Pulsed electric field assisted assembly of polyaniline. *Nanotechnology* **2012**, *23*, 335303-1–335303-10.
- (27) Modi, S.; Wei, M.; Mead, J. L.; Barry, C. M. F. Effect of processing parameters on the electrophoretic deposition of carbon black nanoparticles in moderately viscous systems. *Langmuir* **2011**, *27*, 3166–3173.
- (28) Leblanc, J. L. Rubber-filler interactions and rheological properties in filled compounds. *Prog. Polym. Sci.* **2002**, *27*, 627–687.
- (29) Robertson, C. G.; Lin, C. J.; Rackaitis, M.; Roland, C. M. Influence of particle size and polymer-filler coupling on viscoelastic glass transition of particle-reinforced polymers. *Macromolecules* **2008**, *41*, 2727–2731.
- (30) Choi, S.-S.; Kim, I.-S. Filler–polymer interactions in filled polybutadiene compounds. *Eur. Polym. J.* **2002**, *38*, 1265–1269.
- (31) Leblanc, J. L.; Hardy, P. Evolution of bound rubber during the storage of uncured compounds. *Kautsch. Gummi Kunstst.* **1991**, *44*, 1119–1124.
- (32) Karasek, L.; Sumita, M. Characterization of dispersion state of filler and polymer-filler interactions in rubber-carbon black composites. *J. Mater. Sci.* **1996**, *31*, 281–289.
- (33) Kida, N.; Ito, M.; Yatsuyanagi, F.; Kaido, H. Studies on the structure and formation mechanism of carbon gel in the carbon black filled polyisoprene rubber composite. *J. Appl. Polym. Sci.* **1996**, *61*, 1345–1350.
- (34) Cohen-Addad, J. P. Silica-siloxane mixtures. Structure of the adsorbed layer: chain length dependence. *Polymer* **1989**, *30*, 1820–1823.
- (35) *Vanderbilt Rubber Handbook*, 13th ed.; R. T. Vanderbilt Co.: Norwalk, CT, 1990.
- (36) Scientific Polymer Products Technical Data Sheet, Retrieved from Scientific Polymer Products, Inc. www.scipoly.com (accessed July 15, 2013).
- (37) Sigma-Aldrich Products Technical Data Sheet, Retrieved from Sigma-Aldrich www.sigmaaldrich.com (accessed July 15, 2013).
- (38) Malvern Instrument Technical Note, *Zeta Potential An Introduction in 30 minutes*, Retrieved from Malvern Instrument Ltd. www.malvern.com (accessed July 15, 2013).
- (39) Huckel, E. Die kataphorese der kugel. *Phys. Z* **1924**, *25*, 204.
- (40) Malvern Instrument Frequently Asked Questions, *What Is The Henry Equation?*, Retrieved from Malvern Instrument Ltd. www.malvern.com (accessed July 15, 2013).
- (41) Evans, D. F.; Wennerstrom, H. *The Colloidal Domain, Where Physics, Chemistry, Biology, and Technology Meet*, 2nd ed.; Wiley-VCH: New York, NY, 1999.
- (42) Chand, R. *Chemistry*, 3rd ed.; Random House: New York, NY, 1988.
- (43) Xu, R. L. *Particle Characterization: Light Scattering Methods*; Kluwer Academic Publications: Dordrecht, 2000; pp 223–341.
- (44) Patnaik, A.; Li, C. Evidence for metal interaction in gold metallized polycarbonate films: An x-ray photoelectron spectroscopy investigation. *J. Appl. Phys.* **1998**, *83*, 3049–3056.
- (45) Pantea, D.; Darmstadt, H.; Kaliaguine, S.; Roy, C. Electrical conductivity of conductive carbon blacks: influence of surface chemistry and topology. *Appl. Surf. Sci.* **2003**, *217*, 181–193.
- (46) Darmstadt, H.; Roy, C. Surface spectroscopic study of basic sites on carbon blacks. *Carbon* **2003**, *41*, 2653–2689.
- (47) Donnet, J. B. Filler–elastomer interactions. *Br. Polymer. J.* **1973**, *5*, 213–228.
- (48) Lakdawala, K.; Salovey, R. Rheology of polymers containing carbon black. *Polym. Eng. Sci.* **1987**, *27*, 1035–1042.
- (49) Lei, L.; Yongfeng, S.; Xianhua, C.; Lihua, Q.; Lu, K. Ultrahigh strength and high electrical conductivity in copper. *Science* **2004**, *304*, 422–426.
- (50) Qi, X.-Y.; Yan, D.; Jiang, Z.; Cao, Y.-K.; Yu, Z.-Z.; Yavari, F.; Koratkar, N. Enhanced electrical conductivity in polystyrene nanocomposites at ultra-low graphene content. *Appl. Mater. Interfaces* **2011**, *3*, 3130–3133.
- (51) Donnet, J. B.; Bansal, R. C.; Wang, M. J. *Carbon Black: Science and Technology*, 2nd ed.; New York, 1993.
- (52) Sarkar, P.; De, D.; Rho, H. Synthesis and microstructural manipulation of ceramics by electrophoretic deposition. *J. Mater. Sci.* **2004**, *39*, 819–823.
- (53) Private conversation with Scientific Polymer Products, Inc.
- (54) Billmeyer, F. W. *Textbook of Polymer Science*, 3rd ed.; New York, 1984.
- (55) Wang, H.; Xu, J.-Z.; Zhu, J.-J.; Chen, H.-Y. Preparation of CuO nanoparticles by microwave irradiation. *J. Cryst. Growth* **2002**, *244*, 88–94.
- (56) Jean, J.-H. Electrophoretic deposition of Al₂O₃-SiC composite. *Mater. Chem. Phys.* **1995**, *40*, 285–290.
- (57) Mark, J. E. *Physical Properties of Polymers Handbook*, 2nd ed.; New York, 2006.
- (58) Basu, R. N.; Randall, C. A.; Mayo, M. J. Fabrication of dense zirconia electrolyte films for tubular solid oxide fuel cells by electrophoretic deposition. *J. Am. Ceram. Soc.* **2001**, *84*, 33–40.
- (59) Wang, Y.-C.; Leu, I.-C.; Hon, M.-H. Kinetics of electrophoretic deposition for nanocrystalline zinc oxide coatings. *J. Am. Ceram. Soc.* **2004**, *87*, 84–88.
- (60) Rosseinsky, D. R.; Graham, J. S. Chronoamperometric mobilities in the electrodynamics of a non-aqueous Sol: Depletion, turbulence and electron transfer in sol electrodeposition. *J. Chem. Soc., Faraday Trans.* **1993**, *89*, 3091–3097.